

THE VICTOR–FROG FUNCTION: AN OVERLAP–BASED METRIC ON A QUOTIENT OF VOLUMETRIC SHAPES

VÍCTOR DUARTE MELO

ABSTRACT. Many everyday solids can be continuously deformed into one another, but the informal “amount of effort” required to perform such a deformation depends strongly on how round or sharp the shapes are and on how their volume is distributed. Motivated by informal “clay–model” reasoning about transforming one three–dimensional object into another, we introduce the *Victor–Frog Function* VFF_{3D} . It is a simple, volumetric and target–relative measure of shape similarity which captures how much of the volume of a source object already coincides with a target object after a canonical volume normalisation.

Formally, VFF_{3D} is a Jaccard–type similarity between normalised measurable subsets of \mathbb{R}^3 modulo null sets. We place this construction on a natural quotient space \mathcal{S} of shapes, prove that the associated distance $d_{\text{VF}} = 1 - \text{VFF}_{3D}$ is a genuine metric on \mathcal{S} , and show that the induced metric topology coincides with convergence in measure of the normalised shapes. We also record some elementary invariance properties and a higher–dimensional extension. Finally, we include a small voxel–based numerical experiment comparing an egg–like shape, a cube and a pyramid against a sphere. The goal of this note is not to compete with sophisticated shape analysis frameworks, but to isolate a minimal and mathematically clean version of the underlying intuition.

1. INTRODUCTION

1.1. Origin in informal “clay” deformations. The Victor–Frog Function did not arise from an optimisation problem or from an existing shape analysis pipeline, but from a very simple mental game. The author would imagine that all familiar objects are made of the same homogeneous clay and then, while resting or trying to sleep, mentally *morph* one object into another:

- a mug can be stretched and thickened until it becomes a torus (doughnut);
- an old open padlock feels close, topologically and geometrically, to a rigid “Nokia–era” mobile phone with a visible antenna;
- handcuffs behave like a double torus attached by a short bar;
- an American power socket looks like a pretzel with two holes;
- a baby’s training cup with two handles feels similar to a pair of linked rings;
- and so on, through an endless list of shapes.

Some transformations felt almost effortless: turning an egg into a ball mainly requires smoothing and redistributing volume slightly. Others felt harder: turning a cube into a ball requires rounding off twelve edges and eight corners, and turning a pointed pyramid into a ball felt harder still.

Over many such informal experiments, the author started to rank shapes by how close they felt to a given target such as a sphere or a cube. Crucially, this ranking was not about topological equivalence—all simply connected solids are homeomorphic to a ball—but about *how much of the clay already sits in the right place* when one tries to match the source object to the target.

1.2. Desired properties. Translating this informal game into mathematics suggests that a useful similarity between solids $A, B \subset \mathbb{R}^3$ should satisfy at least the following:

- (1) it should compare *volumes*, not only surfaces, because clay lives in the interior of objects;

2020 *Mathematics Subject Classification.* 28A75, 52A38, 54E35, 68U05.

Key words and phrases. shape similarity, Jaccard index, geometric measure theory, convergence in measure, voxel approximation.

- (2) it should be independent of the choice of orientation, i.e. invariant under global rotations of the coordinate system; translations can be absorbed into a convenient choice of origin or into an aligned variant;
- (3) it should be insensitive to global rescaling: only the shape matters, not the absolute size;
- (4) it should be *relative* to a chosen target B (“how spherical?”, “how cubic?”, and so on);
- (5) it should be normalised to $[0, 1]$, with value 1 only when the shapes coincide (up to negligible discrepancies);
- (6) it should be simple enough to compute numerically on voxel grids.

The construction presented below achieves all of these goals by combining a very simple volume normalisation with the classical Jaccard similarity of sets [1].

2. THE SHAPE SPACE AND NORMALISATION

We work in Euclidean three-space \mathbb{R}^3 equipped with the standard Lebesgue measure \mathcal{L}^3 , which we informally call “volume”. A *shape* will be any measurable subset $A \subset \mathbb{R}^3$ with finite, strictly positive volume $\mathcal{L}^3(A) \in (0, \infty)$.

We shall systematically identify shapes that agree up to Lebesgue–null sets. More precisely, we write $A \sim B$ if $\mathcal{L}^3(A \Delta B) = 0$, where $A \Delta B = (A \setminus B) \cup (B \setminus A)$ denotes the symmetric difference, and we work on the quotient space

$$\mathcal{S} = \{A \subset \mathbb{R}^3 : 0 < \mathcal{L}^3(A) < \infty\}/\sim.$$

All statements below are understood modulo this identification.

Two geometric operations play a central role:

- **Rotations:** transformations of the form $x \mapsto Rx$, where $R \in SO(3)$ is a rotation matrix;
- **Uniform scaling:** transformations of the form $x \mapsto sx$ with a scalar $s > 0$.

Rotations preserve volume exactly, while uniform scaling multiplies volume by s^3 . In order to compare shapes independently of their absolute size, we introduce a canonical volume normalisation.

Definition 2.1 (Volume normalisation). Let $A \subset \mathbb{R}^3$ be a shape with volume $\mathcal{L}^3(A) > 0$. Its *normalised version* \tilde{A} is defined by

$$\tilde{A} = s_A A \quad \text{with} \quad s_A = \mathcal{L}^3(A)^{-1/3}.$$

Then $\mathcal{L}^3(\tilde{A}) = 1$.

Remark 2.1. The volume normalisation is well defined on the quotient space \mathcal{S} : if $A \sim B$, then $\mathcal{L}^3(A) = \mathcal{L}^3(B)$, so $s_A = s_B$, and the scaled sets $\tilde{A} = s_A A$ and $\tilde{B} = s_B B$ also satisfy $\mathcal{L}^3(\tilde{A} \Delta \tilde{B}) = 0$.

Thus every shape is rescaled to unit volume, so that the comparison depends only on the distribution of mass and not on total size.

3. THE VICTOR–FROG FUNCTION

Intuitively, the portion of volume where the normalised shapes \tilde{A} and \tilde{B} already coincide is the mass that does *not* need to be moved when deforming A into B (after global normalisation). The union $\tilde{A} \cup \tilde{B}$ represents the region potentially occupied by either shape. This leads directly to the following definition.

Definition 3.1 (Victor–Frog Function in 3D). Let $A, B \subset \mathbb{R}^3$ be shapes with $0 < \mathcal{L}^3(A), \mathcal{L}^3(B) < \infty$, and let \tilde{A}, \tilde{B} denote their normalised versions of unit volume. The *Victor–Frog Function in dimension three* is

$$\text{VFF}_{3D}(A, B) = \frac{\mathcal{L}^3(\tilde{A} \cap \tilde{B})}{\mathcal{L}^3(\tilde{A} \cup \tilde{B})}.$$

At the level of sets, $\text{VFF}_{3D}(A, B)$ is exactly the Jaccard similarity coefficient of the normalised shapes [1, 2], but here the emphasis is on the concrete geometric interpretation: the numerator is the volume that already matches, and the denominator is the total volume that could possibly be occupied by either object after normalisation.

The function VFF_{3D} is symmetric in A and B ; however, in many applications one fixes a target shape B (for instance, a sphere or a cube) and interprets $\text{VFF}_{3D}(A, B)$ as “how close A already is to B ” in the sense of minimal clay movement.

One may optionally refine the definition by allowing a best rigid alignment of the shapes before measuring overlap. By a rigid motion we mean a map

$$x \mapsto Rx + t, \quad R \in SO(3), t \in \mathbb{R}^3.$$

Rigid motions preserve Lebesgue measure and send shapes to shapes within the same equivalence class of \mathcal{S} .

Definition 3.2 (Aligned Victor–Frog Function). Let \mathcal{G} denote the group of rigid motions of \mathbb{R}^3 . The *aligned* Victor–Frog Function is

$$\text{VFF}_{3D}^{\text{alg}}(A, B) = \sup_{g \in \mathcal{G}} \frac{\mathcal{L}^3(g(\tilde{A}) \cap \tilde{B})}{\mathcal{L}^3(g(\tilde{A}) \cup \tilde{B})}.$$

In the rest of this note we work with the simpler non-aligned version VFF_{3D} , but all basic properties below also hold for $\text{VFF}_{3D}^{\text{alg}}$.

4. BASIC PROPERTIES

We now record a few elementary facts which justify the interpretation of VFF_{3D} as a shape similarity measure and as a normalised “inverse deformation energy”.

Proposition 4.1 (Range and extremal cases). *For any shapes $A, B \subset \mathbb{R}^3$ with positive finite volume,*

$$0 \leq \text{VFF}_{3D}(A, B) \leq 1.$$

Moreover:

- $\text{VFF}_{3D}(A, B) = 1$ if and only if \tilde{A} and \tilde{B} agree up to a set of Lebesgue measure zero;
- $\text{VFF}_{3D}(A, B) = 0$ if and only if $\mathcal{L}^3(\tilde{A} \cap \tilde{B}) = 0$, i.e. they are disjoint up to measure zero.

Proof. Since $\tilde{A} \cap \tilde{B} \subset \tilde{A} \cup \tilde{B}$, monotonicity of \mathcal{L}^3 yields $\mathcal{L}^3(\tilde{A} \cap \tilde{B}) \leq \mathcal{L}^3(\tilde{A} \cup \tilde{B})$, so the ratio lies in $[0, 1]$ whenever the denominator is positive. But $\mathcal{L}^3(\tilde{A}) = \mathcal{L}^3(\tilde{B}) = 1$ implies $\mathcal{L}^3(\tilde{A} \cup \tilde{B}) \geq 1$, hence the denominator is indeed strictly positive.

If $\tilde{A} = \tilde{B}$ up to a null set, then $\tilde{A} \cap \tilde{B} = \tilde{A} \cup \tilde{B}$ up to a null set, so the ratio is 1. Conversely, if the ratio is 1, then $\mathcal{L}^3(\tilde{A} \cup \tilde{B} \setminus \tilde{A} \cap \tilde{B}) = 0$, hence the symmetric difference has measure zero and the sets agree almost everywhere. The characterisation of $\text{VFF}_{3D} = 0$ is immediate. \square

Proposition 4.2 (Symmetry). *For any shapes A, B ,*

$$\text{VFF}_{3D}(A, B) = \text{VFF}_{3D}(B, A).$$

Proof. Interchanging A and B simply interchanges \tilde{A} and \tilde{B} . Since intersection and union are symmetric operations, $\tilde{A} \cap \tilde{B} = \tilde{B} \cap \tilde{A}$ and $\tilde{A} \cup \tilde{B} = \tilde{B} \cup \tilde{A}$, the ratio is unchanged. \square

Proposition 4.3 (Invariance under common rotations). *Let $R \in SO(3)$ be a rotation about the origin, and let $A' = RA$, $B' = RB$. Then*

$$\text{VFF}_{3D}(A', B') = \text{VFF}_{3D}(A, B).$$

Proof. Rotations preserve Lebesgue measure and do not change volumes, so $\mathcal{L}^3(A') = \mathcal{L}^3(A)$ and $\mathcal{L}^3(B') = \mathcal{L}^3(B)$. Hence the normalisation factors s_A, s_B are the same for A, B and for A', B' . The normalised shapes satisfy $\tilde{A} = s_A A$, $\tilde{B} = s_B B$, and $\tilde{A}' = s_A A' = s_A R A = R(s_A A) = R\tilde{A}$, with an analogous identity $\tilde{B}' = R\tilde{B}$. Therefore

$$\tilde{A}' \cap \tilde{B}' = R(\tilde{A} \cap \tilde{B}), \quad \tilde{A}' \cup \tilde{B}' = R(\tilde{A} \cup \tilde{B}).$$

Applying \mathcal{L}^3 and using the fact that R is measure-preserving yields $\mathcal{L}^3(\tilde{A}' \cap \tilde{B}') = \mathcal{L}^3(\tilde{A} \cap \tilde{B})$ and similarly for the union, so the defining ratio of VFF_{3D} is unchanged. \square

Proposition 4.4 (Invariance under common scaling). *Let $c > 0$ and define $A_c = cA$, $B_c = cB$. Then*

$$\text{VFF}_{3D}(A_c, B_c) = \text{VFF}_{3D}(A, B).$$

Proof. Uniform scaling by c multiplies volume by c^3 , hence $\mathcal{L}^3(A_c) = c^3 \mathcal{L}^3(A)$ and $\mathcal{L}^3(B_c) = c^3 \mathcal{L}^3(B)$. The normalisation factor for A_c is $s_{A_c} = \mathcal{L}^3(A_c)^{-1/3} = (c^3 \mathcal{L}^3(A))^{-1/3} = c^{-1} s_A$, and similarly $s_{B_c} = c^{-1} s_B$. Therefore $\tilde{A}_c = s_{A_c} A_c = c^{-1} s_A c A = \tilde{A}$, and likewise $\tilde{B}_c = \tilde{B}$. The formula for VFF_{3D} is therefore unchanged. \square

It is also natural to consider the associated *Victor–Frog distance*

$$d_{\text{VF}}(A, B) = 1 - \text{VFF}_{3D}(A, B),$$

which vanishes precisely when the normalised shapes coincide almost everywhere. Up to the normalisation step, d_{VF} is exactly the classical Jaccard distance between measurable sets, which is known to satisfy the triangle inequality on equivalence classes modulo null sets [2]. Thus d_{VF} defines a genuine metric on the quotient space \mathcal{S} of shapes modulo Lebesgue-null sets.

4.1. Topology induced by d_{VF} . Since all normalised shapes satisfy $\mathcal{L}^3(\tilde{A}) = 1$, the union $\tilde{A} \cup \tilde{B}$ always has volume in $[1, 2]$. Moreover, for any shapes A, B we have the identity

$$\mathcal{L}^3(\tilde{A} \Delta \tilde{B}) = \mathcal{L}^3(\tilde{A} \cup \tilde{B}) - \mathcal{L}^3(\tilde{A} \cap \tilde{B}),$$

which immediately relates d_{VF} to the measure of the symmetric difference.

Proposition 4.5 (Equivalence with convergence in measure). *Let $(A_n)_{n \geq 1}$ be a sequence of shapes and let A be another shape. Denote by \tilde{A}_n and \tilde{A} their normalised versions. Then the following are equivalent:*

- (1) $d_{\text{VF}}(A_n, A) \rightarrow 0$ as $n \rightarrow \infty$;
- (2) $\mathcal{L}^3(\tilde{A}_n \Delta \tilde{A}) \rightarrow 0$ as $n \rightarrow \infty$.

In particular, the metric topology induced by d_{VF} on \mathcal{S} coincides with the topology induced by convergence in measure of the normalised shapes.

Proof. Write $U_n = \tilde{A}_n \cup \tilde{A}$ and $I_n = \tilde{A}_n \cap \tilde{A}$. Then

$$\mathcal{L}^3(\tilde{A}_n \Delta \tilde{A}) = \mathcal{L}^3(U_n) - \mathcal{L}^3(I_n),$$

and by definition

$$d_{\text{VF}}(A_n, A) = 1 - \frac{\mathcal{L}^3(I_n)}{\mathcal{L}^3(U_n)} = \frac{\mathcal{L}^3(U_n) - \mathcal{L}^3(I_n)}{\mathcal{L}^3(U_n)} = \frac{\mathcal{L}^3(\tilde{A}_n \Delta \tilde{A})}{\mathcal{L}^3(U_n)}.$$

Since $\mathcal{L}^3(\tilde{A}_n) = \mathcal{L}^3(\tilde{A}) = 1$ for all n , we always have $1 \leq \mathcal{L}^3(U_n) \leq 2$. Thus

$$\frac{1}{2} \mathcal{L}^3(\tilde{A}_n \Delta \tilde{A}) \leq d_{\text{VF}}(A_n, A) \leq \mathcal{L}^3(\tilde{A}_n \Delta \tilde{A}),$$

and the claimed equivalence follows immediately. \square

Remark 4.1. Proposition 4.5 shows that (\mathcal{S}, d_{VF}) is a bounded metric space whose topology agrees with the usual convergence in measure for normalised shapes. In particular, questions of completeness, compactness or stability for VFF_{3D} may be studied within the well-developed framework of metric measure spaces.

Remark 4.2 (Higher-dimensional extension). All definitions and proofs above extend verbatim to \mathbb{R}^n for any $n \geq 1$ upon replacing \mathcal{L}^3 by the n -dimensional Lebesgue measure \mathcal{L}^n and using the normalisation factor $s_A = \mathcal{L}^n(A)^{-1/n}$. In that setting the resulting function VFF_{nD} provides an overlap-based similarity for n -dimensional volumetric shapes.

5. A VOXEL-BASED APPROXIMATION

5.1. Discrete construction. For computational purposes, a natural approximation of VFF_{3D} uses 3D voxel grids.

Definition 5.1 (Voxel Victor–Frog approximation). Fix a bounded box in \mathbb{R}^3 and subdivide it into N^3 congruent voxels for some resolution $N \in \mathbb{N}$. For a shape A , mark a voxel as belonging to A if its centre lies in A . Denote by n_A the number of voxels marked for A . The *voxel-normalised* version of A is obtained by applying a uniform scaling with factor

$$s_A = \left(\frac{n_\star}{n_A} \right)^{1/3},$$

where n_\star is a chosen reference count (for instance, the average of the n_A across all shapes under comparison). After this scaling, all shapes have approximately the same discrete volume.

Let $n_{A \cap B}$ and $n_{A \cup B}$ denote, respectively, the number of voxels belonging to the intersection and union of the normalised discrete shapes. The *voxel Victor–Frog approximation* is

$$VFF_{3D}^{\text{vox}}(A, B) = \frac{n_{A \cap B}}{n_{A \cup B}}.$$

As the resolution N tends to infinity and the box expands so as to contain the support of the normalised shapes, one expects $VFF_{3D}^{\text{vox}}(A, B)$ to approach the theoretical $VFF_{3D}(A, B)$ under standard regularity assumptions on the shapes, in the usual sense of voxel-based approximations of volume.

5.2. Example: sphere vs. egg, cube and pyramid. To match the original mental experiments behind the Victor–Frog Function, we consider a simple numerical example where the target B is a sphere and the source A is, in turn, an egg-like ellipsoid, a cube and a right square pyramid.

On a regular grid with $N = 80$ in a box $[-1.8, 1.8]^3$, we define:

- a unit sphere centred at the origin: $A_{\text{sphere}} = \{(x, y, z) : x^2 + y^2 + z^2 \leq 1\}$;
- an egg-like ellipsoid, $A_{\text{egg}} = \left\{ (x, y, z) : \left(\frac{x}{a}\right)^2 + \left(\frac{y}{b}\right)^2 + \left(\frac{z-\delta}{c}\right)^2 \leq 1 \right\}$ with $(a, b, c, \delta) = (1.0, 0.9, 1.1, 0.15)$;
- a cube $A_{\text{cube}} = \{(x, y, z) : |x| \leq 1, |y| \leq 1, |z| \leq 1\}$;
- a right square pyramid with base at $z = -1$ and apex at $z = 1$, defined by $A_{\text{pyr}} = \{(x, y, z) : -1 \leq z \leq 1, \max(|x|, |y|) \leq (1-z)/2\}$.

We first estimate raw discrete volumes by counting voxels for each shape, then apply the voxel normalisation described above so that all shapes occupy roughly the same number of voxels. Finally, we compute $VFF_{3D}^{\text{vox}}(A, B)$ with B fixed as the sphere. A simple Python/NumPy implementation (not included here for space reasons) yields the indicative values in Table 1.

Figure 1 shows these values as a simple bar chart, suitable for quick comparison or as a diagnostic plot when experimenting with other families of shapes.

Pair (A, B)	Approximate $\text{VFF}_{3D}^{\text{vox}}(A, B)$
egg vs. sphere	0.78
cube vs. sphere	0.72
pyramid vs. sphere	0.34

TABLE 1. Approximate voxel Victor–Frog similarities $\text{VFF}_{3D}^{\text{vox}}(A, B)$ at resolution $N = 80$ on a box $[-1.8, 1.8]^3$. As expected, the egg–like shape is closest to the sphere, the cube is somewhat less spherical, and the sharp pyramid is substantially further away.

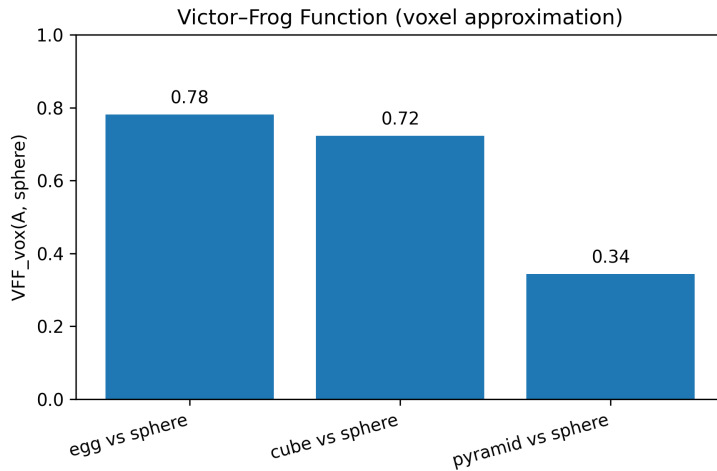


FIGURE 1. Illustrative comparison of $\text{VFF}_{3D}^{\text{vox}}(A, B)$ for three shapes A (egg–like, cube, pyramid) against a spherical target B . The actual values depend on grid resolution, but the qualitative ordering is robust.

6. RELATED WORK

The underlying set–theoretic quantity in VFF_{3D} is the classical Jaccard similarity, introduced in [1] and studied from a metric viewpoint in [2]. In shape analysis and computer vision, a wide range of other distances are used, such as the Hausdorff distance between boundaries [3] and various level–set and signed–distance based methods [4, 5].

Compared to these, the Victor–Frog Function deliberately trades geometric detail for simplicity: it works purely with volumetric overlap after a canonical normalisation and can be implemented on voxels with a few lines of code, while still producing values that align well with intuitive judgements such as “egg closer to ball than cube, and cube closer to ball than pyramid”. It may thus serve as a minimal baseline or a sanity check when developing more elaborate metrics.

7. CONCLUDING REMARKS

The Victor–Frog Function VFF_{3D} formalises, in a very compact formula, the intuition that “*the closer two solids already overlap in space, the less energy is required to deform one into the other*”. It uses only basic measure theory, is invariant under global rotations and global scaling, and yields a dimensionless similarity value in $[0, 1]$ which is tightly aligned with human geometric intuition. Its aligned variant $\text{VFF}_{3D}^{\text{alg}}$ is, by construction, insensitive to full rigid motions of the underlying shapes.

Several natural extensions suggest themselves:

- the definition and all proofs carry over verbatim to \mathbb{R}^n for $n \geq 1$;
- one may combine VFF_{3D} with curvature-based penalties to distinguish between very sharp and very smooth boundaries when the volumetric overlap is similar;
- the aligned version VFF_{3D}^{alg} can be combined with numerical optimisation over rigid motions to factor out pose differences when comparing shapes extracted from data.

Even in its simplest three-dimensional form, however, the Victor–Frog Function already provides a clean and mathematically well-founded tool to quantify “minimal deformation energy” between volumetric shapes.

REFERENCES

- [1] P. Jaccard. *Étude comparative de la distribution florale dans une portion des Alpes et du Jura*. Bulletin de la Société Vaudoise des Sciences Naturelles, 37:547–579, 1901.
- [2] J. C. Gower and P. Legendre. Metric and Euclidean Properties of Dissimilarity Coefficients. *Journal of Classification*, 3:5–48, 1986.
- [3] F. Hausdorff. *Grundzüge der Mengenlehre*. Leipzig: Veit, 1914.
- [4] S. Osher and R. Fedkiw. *Level Set Methods and Dynamic Implicit Surfaces*. Springer, 2003.
- [5] A. M. Bronstein, M. M. Bronstein, and R. Kimmel. *Numerical Geometry of Non-Rigid Shapes*. Springer, 2008.

INDEPENDENT RESEARCHER

Email address: victormeloasm@gmail.com